LINEAR AND NON-LINEAR CALCULATIONS OF THE HOSE INSTABILITY IN THE ION-FOCUSED REGIME*

UCID--19495

DE82 021549

H. Lee Buchanan

June 14, 1982

Lawrence Livermore National Laboratory

University of California

Livermore, California 94550

ABSTRACT

A simple model is adopted to study the hose instability of an intense relativistic electron beam in a partially neutralized, low density ion channel (ion focused regime). Equations of motion for the beam and the channel are derived and linearized to obtain an approximate dispersion relation. The non-linear equations of motion are then solved numerically and the results compared to linearized data.

*Lawrence Livermore National Laboratory is operated by the University of California for the U. S. Department of Energy under Contract No. W-7405-Eng-48.

This work is performed by LLNL for the U. S. Department of Defense under DARPA (DOD) ARPA Order No. 4395 Amendment No. 1, monitored by NSWC under document number N60921-82-WR-W0056.

I. Introduction

An intense relativistic electron beam will propagate through a gas in self-pinch equilibrium if the gas is ionized and a sufficient number of free electrons can escape from the region of the beam so that the radial electric field of the beam is neutralized. When this occurs, the self-magnetic pinch force of the beam can exceed the combination of the outward directed radial electrostatic force and the transverse beam particle temperature (emittance) and a transverse steady state is established. Briggs and Yu[1] have recently examined two limiting extremes of this charge neutralization process which they term the "local conductivity approximation" (LCA) and the "ion focused regime" (IFR). In LCA the mean free path of plasma electrons is very short and the usual collisional concept of conductivity is valid. In the IFR, however, gas density is very low so that secondary electrons produced by primary impact ionization of the background gas by beam electrons are expelled radially causing insignificant ionization. For this case, the approximation can often be made that these electrons leave instantaneously. When valid, this assumption greatly simplifies the theory.

Interest in the IFR has evolved chiefly from the experimental observation that within a certain pressure range, typically 20 - 50 microns in hydrogen, a 5 MeV, 300 amp electron beam exhibits stable propagation over considerable distances. This "low pressure window" has great potential as a propagating environment for certain applications including beam pulse conditioning cells and long distance beam transport.

In the typical IFR experiment, the beam is introduced into an unionized low density gas. Ionization builds up due to collisions between beam electrons and gas atoms and by avalanche ionization in the gas due to the very strong radial electric (space charge) and axial electric (inductive) fields associated with the pulse head. In this report, however, we consider a situation in which the gas is ionized to some fraction f_n of the beam current just prior to the entry of the beam. This is accomplished by some external means such as another particle beam or a laser. The beam then sees a cylindrical channel of charge neutral gas, ionized to a fraction of $f_n = n_i/n_b$ where n_i is the ion density and n_b is the beam electron density. Plasma electrons immediately leave the channel when the beam enters due to the radial electric field E_r and the massive ions remain behind partially neutralizing the space charge of the beam particles.

II. A Simple Model

If we assume that the background ion density is less than the beam density, $n_i \leq n_b \cong I_b/a^2$ $(f_n \leq 1)$ where a is the beam radius, that the beam itself contributes insignificant further ionization, and that the plasma electrons move far away from the beam/channel system before colliding with background gas, a simple one-dimensional model of transverse beam dynamics can be applied.

We now look at a system comprised of an azimuthally symmetric beam of current I_b, which contains $N_b = I_b/ec$ particles per unit length, and an azimuthally symmetric channel of ions which number $f_n N_b$ per unit length.

The beam particles, here relativistic electrons, have a mass γm_e where γ is the usual relativistic factor and m_e is the electron mass, while the ions have a mass m_i. The transverse position of the beam and channel are allowed to vary and are measured with respect to the original coaxial position of the beam/channel system. We have depicted the beam and the channel in cross section below with d representing the transverse displacement of the channel and y denoting the transverse displacement of the beam.

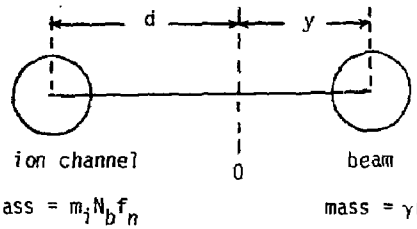

For simplicity, we take the radius of both the beam and the channel to be a and note that initially $d = y = 0$.

The beam and the channel will, of course, attract one another since they are of opposite sign, the precise force law depending on the radial profile. Certain features of the force law, however, will be common to most physically reasonable profiles (monotonically decreasing with increasing r and zero slope at $r = 0$). If, for instance, the beam and channel are separated by a distance Δ that is small, $\Delta^2 << 2a^2$, and transverse profiles of the beam and channel are the same, then the force law can be shown to be

$$\left|\text{force/unit length}\right| = \frac{I^2}{c^2}\,\frac{\Delta}{a^2}\,, \qquad (1)$$

where I is the beam current and c is the speed of light. On the other hand, if $\Delta^2 >> 2a^2$ the force law is

$$\left|\text{force/unit length}\right| = \frac{I^2}{c^2}\,\frac{2}{\Delta}\,, \tag{2}$$

which is just the force law for two line charges. A simple function which has these two limiting values is

$$\left|\text{force/unit length}\right| = \frac{I^2}{c^2}\left[\frac{\Delta}{a^2 + \tfrac{1}{2}\Delta^2}\right]. \tag{3}$$

Since we are interested in the qualitative features of beam/channel motion rather than features specific to a particular profile, Equation (3) will be taken as our force law for this study.

The equations of motion for the beam and the channel then follow immediately as

$$\gamma m_e N_b\, \ddot{y} = -\, f_n\, \frac{I_b^2}{c^2}\left[\frac{(y - d)}{a^2 + \tfrac{1}{2}(y - d)^2}\right] \tag{4}$$

$$f_n m_i N_b\, \ddot{d} = f_n\, \frac{I_b^2}{c^2}\left[\frac{(y - d)}{a^2 + \tfrac{1}{2}(y - d)^2}\right], \tag{5}$$

respectively. We now introduce a variable $x = ct - z$ where z is the distance that the beam travels in the direction of its propagation. Note that x may be used to label a particle or moving beam segment since it (times c) is the time of injection at $z = 0$ ($v_z = c$). For the transformation we have the identities

$$\left.\frac{\partial}{\partial t}\right|_z = c \left.\frac{\partial}{\partial x}\right|_z$$

$$\left.\frac{\partial}{\partial z}\right|_t = \left.\frac{\partial}{\partial z}\right|_x - \left.\frac{\partial}{\partial x}\right|_z .$$

If we further define

$$Y = \frac{y}{a} ; \quad D = \frac{d}{a} ; \quad I_A = \frac{\beta\gamma mc^3}{q}$$

$$Z^2 = f_n \frac{z^2}{a^2} \frac{I_b}{I_A} ; \quad X^2 = \frac{x^2}{a^2} \frac{m_e}{m_i} \frac{I_b}{I_A} ,$$

we immediately obtain the dimensionless equations of motion

$$\frac{\partial^2}{\partial Z^2} Y = - \frac{(Y - D)}{1 + \frac{1}{2}(Y - D)^2} \tag{6}$$

$$\frac{\partial^2}{\partial X^2} D = \frac{(Y - D)}{1 + \frac{1}{2}(Y - D)^2} . \tag{7}$$

Note that $Y = D = 0$ is identically a solution and will constitute an equilibrium propagation state.

III. Low Frequency Hose

We first consider the system's response to a transverse displacement of the beam with respect to the channel. If this displacement is very small, $D, Y << 1$, then Equations (6) and (7) can be linearized to obtain

$$\frac{\partial^2}{\partial Z^2} Y = D - Y \tag{8}$$

$$\frac{\partial}{\partial X^2} D = Y - D \quad . \tag{9}$$

If we then assume a form for Y and D

$$Y \sim D \sim \exp\left[-(iKX + i\Omega Z)\right] \quad ,$$

then Equations (8) and (9) yield a dispersion relation

$$D(\Omega,K) = (1 - \Omega^2)(1 - K^2) - 1 = 0 \quad , \tag{10}$$

where Ω and K are dimensionless wave numbers. From this dispersion relation, taking K to be real, we see that a resonance appears at $K = 1$ and that instability occurs for $K \leq 1$. This is the simple hose instability in which transverse oscillations of the beam and the channel couple and grow. The instability is convective since the point of maximum growth is not stationary in either the beam or the channel frame, but moves with a dimensionless group velocity

$$\frac{d\Omega}{dK} = \frac{2K}{(1 + K^2)^2} \quad . \tag{11}$$

We are most interested in finding is the growth rate of the instability in its own frame which can be obtained from the impulse response of the system

$$\begin{aligned} G(X,Z) &= \frac{1}{2\pi}\int d\Omega \int dK \; \frac{e^{i(KX + \Omega Z)}}{D(\Omega,K)} \\ &= \frac{1}{2\pi}\int d\Omega \int dK \; \exp\left[i(KX + \Omega Z) - \ell n\, D\right] . \end{aligned} \tag{12}$$

Explicit calculation of this integral is difficult, but we can easily evaluate the asymptotic form of the growth by performing a saddle point calculation. First, let us call the exponent in Equation (12) $g(\Omega,K)$. The saddle then occurs where

$$\frac{\partial g}{\partial \Omega} = 0 \quad \text{and} \quad \frac{\partial g}{\partial K} = 0$$

or

$$iZD - \frac{\partial D}{\partial \Omega} = 0 \quad \text{and} \quad iXD - \frac{\partial D}{\partial K} = 0 \ . \tag{13}$$

We define $V = X/Z$ and obtain from (13)

$$D_K - VD_\Omega = 0 \ , \tag{14}$$

where the subscript denotes partial differentiation with respect to the subscripted variable. If we now solve Equations (14) and (10) for Ω and K the growth can be found as

$$G(X,Z) \qquad \exp\left[\mathrm{Im}\,(\Omega - KV)Z\right] \ . \tag{15}$$

A more rigorous derivation of Equation (15) has been done by E. Lee using Lagrange multiplier formalism.[3]

Now in our case, Equations (14) and (10) yield

$$K^2 = 1 + \left(-\frac{Z}{X}\right)^{2/3}$$

$$\Omega^2 = 1 + \left(-\frac{X}{Z}\right)^{2/3} \ ,$$

which can be simplified if we restrict ourselves to $Z/X >> 1$, i.e., long propagation distances.

Then

$$K \approx \left(-\frac{Z}{X}\right)^{1/3}\left[1+\frac{1}{2}\left(-\frac{X}{Z}\right)^{2/3}\right]$$

$$\approx 1+\frac{1}{2}\left(-\frac{X}{Z}\right)^{2/3},$$

and finally

$$G(X,Z) \qquad \exp\left[\frac{\sqrt{3}}{4}\left(X^2Z\right)^{1/3}\right]. \tag{16}$$

Clearly the instability grows without bound with increasing X and Z, a consequence of the rigid beam/channel modeling of Equations (4) and (5) and the infinite resonance that results. The assumption of rigidity while simplifying the analysis is quite unphysical except at low frequencies and as we see in the next section, it obscures important physical phenomena.

IV. Spread Mass Modeling

As outlined in reference 2, there is compelling evidence to the introduction of a large spread in betatron frequencies. Physically, this spread derives from the fact that the transverse potential well which contains beam particles is anharmonic. Particles localized near the axis oscillate with a frequency greater than particles which are able to move to the outer edge of the profile. This spread has the effect of introducing a maximum frequency above which the instability is damped. To incorporate betatron frequency spreading into our model, we adopt the spread mass model of E. P. Lee.[2]

The real beam is considered to behave as if each longitudinal segment is composed of many rigid disks having the same transverse charge density profile as the beam, but with varying mass. The same arguments can be made for the channel ions since we have previously assumed that the channel and beam profiles are the same. A continuous variable η is defined which serves as a subscript label for the disks within a segment such that $0 \leq \eta \leq 1$. To proceed we must select the radial form for the transverse charge density profile. Selecting the Bennett profile

$$J(r) \propto \frac{1}{(1 + r^2/a^2)^2} \quad , \tag{17}$$

then $\Omega_{max} = 2$ in normalized units corresponds to the betatron frequency of particles near the axis. All other particles have smaller betatron frequencies which are distributed as

$$\Omega_\eta = \eta\Omega_{max} = 2\eta \quad . \tag{18}$$

The displacement of a beam segment is the weighted mean of all of the disks

$$Y = \int_0^1 d\eta \, w(\eta) \, Y_\eta \quad , \tag{19}$$

Lee has shown[2] that the normalized weighting function $w(\eta)$ that is appropriate to the Bennett is

$$w(\eta) = 6\eta(1 - \eta) \quad . \tag{20}$$

Adopting these ideas, we can modify the linearized Equations (8) and (9) to get

$$\frac{\partial^2}{\partial Z^2} Y_\eta = 2\eta (\bar{D} - Y_\eta) \tag{21}$$

$$\frac{\partial^2}{\partial X^2} D_\xi = 2\xi (\bar{Y} - D_\xi) \quad . \tag{22}$$

Note here that we have explicitly spread the mass of the channel (with index ξ) as well as the beam (with index η). For the channel, the mean displacement $\bar{D}$ is calculated exactly as Equation (19) with the weighting function of Equation (20). Using the same form of perturbation as before, the new dispersion relation becomes

$$1 = \int_0^1 d\xi\, w(\xi)\, \frac{2\xi}{(2\xi - K^2)} \int_0^1 d\eta\, w(\eta)\, \frac{2\eta}{(2\eta - \Omega^2)} \quad . \tag{23}$$

It is easy to see that using a single disk approximation where $w(\alpha) = \delta(\alpha - \frac{1}{3})$ reproduces Equation (10). To compute the integrals of Equation (23) we substitute relation (20) for $w(\eta)$ to obtain

$$I(\alpha) = 6 \int_0^1 du\, u^2\, \frac{(1-u)}{(u-\alpha)}$$

$$= 1 + 3\alpha - 6\alpha^2 \left\{ 1 - (1-\alpha) \left[\pi i + \ell n \left(\frac{1-\alpha}{\alpha} \right) \right] \right\},$$

noting that the imaginary component arises from the pole at $u = \alpha$. The dispersion relation is finally

$$I = I(K^2/2)\, I(\Omega^2/2) \quad . \tag{24}$$

This expression is difficult to analyze in general, so we shall study the character of the instability by numerically solving Equations (21) and (22).

V. Linearized Computational Model

A simple code has been constructed to solve numerically Equations (21) and (22). The continuum of beam disks (indexed η) and the continuum of channel disks (indexed ξ) have been replaced by a set of N disks evenly spaced in the variable η and ξ. The equations are then differenced and become

$$\begin{aligned}
U_i^{n+\frac{1}{2}} - U_i^{n-\frac{1}{2}} &= 2i\Delta Z\, w_i\, (\bar{D} - Y_i)/N \\
Y_i^{n+1} - Y_i^{n} &= \Delta Z\, U_i^{n+\frac{1}{2}} \\
V_j^{m+\frac{1}{2}} - V_j^{m-\frac{1}{2}} &= 2j\Delta X\, w_j\, (\bar{Y} - D_j)/N \\
D_j^{m+1} - D_j^{m} &= \Delta X\, V_j^{m+\frac{1}{2}} \quad ,
\end{aligned} \tag{25}$$

where n is the index assigned tc the Z-step and m is the index denoting the X-step. The averaged quantities are defined as

$$\bar{Q} = \sum_{i=1}^{N} f_i\, Q_i \quad , \tag{26}$$

where in all of the above

$$w_i = \frac{i - \frac{1}{2}}{N} \tag{27}$$

and $$f_i = \left(1 + \frac{1}{2N^2}\right)^{-1} \frac{6}{N} w_i (1 - w_i) \quad .$$

The spread mass model is nearly identical to that originally due to E. P. Lee[2] which has the feature that

$$\sum_{i=1}^{N} f_i = 1$$

$$\sum_{i=1}^{N} f_i / w_i = 3 + \mathcal{O}(N^2) \quad .$$

The feature new to this work is that <u>both</u> the channel <u>and</u> the beam have mass spreading with the number of disks the same for each.

The code was run for $N = 50$ and the results are not qualitatively dissimilar to previous codes. First we note that $\bar{Y} = \bar{D} = \text{const}$, $U_i^0 = V_j^0 = 0$ is a solution showing that spatial invariance is retained. This provides an important numerical check. If we let $U_i^0 = V_j^0 = D^0 = 0$ and perturb $\bar{Y}^0$ with a step function H or

$$\bar{Y}^0(X) = H(X - X_0) \quad , \tag{28}$$

then the results are as depicted in Figure 1 where $X_p = 2$. The perturbation of the initial disk damps away with increasing Z due to phase mixing. At larger values of X the perturbation initially grows, reaches a maximum, and then damps away reflecting the convective nature of the instability. It is

characteristic that as X increases, the saturated growth increases and the position Z of the saturation also increases. If one plots $\bar{Y}_{max}$ as a function of X one obtains Figure 2 showing pure exponential growth of the form

$$\bar{Y}_{max} \propto e^{p(X - X_o)} \tag{29}$$

where X_o is the point in X at which the perturbation is applied. From Figure 2 we calculate $p = 1.54$. The position Z at which the saturation occurs is obtained from Figure 3 where we have plotted $Z(\bar{Y}_{max})$ vs. X. A group velocity may be calculated to be

$$\frac{\Delta X}{\Delta Z} = .379 \quad . \tag{30}$$

It is useful to rewrite Equation (29) in un-normalized coordinates for the length in x required for e-folding

$$x - x_o = .65\, a \left(\frac{17}{I_b(kA)} \frac{m_i}{m_e}\right)^{\frac{1}{2}} \quad . \tag{31}$$

This distance is <u>independent</u> of beam energy and ion density and only weakly dependent on beam current. The instability is convective so that to obtain the propagated distance $(z - z_p)$ for e-folding, we must apply the group velocity (30).

$$(z - z_p) = 2.64 \left(\frac{m_e}{m_i} \frac{\gamma}{f_n}\right)^{\frac{1}{2}} (x - x_o)$$

$$= 1.71\, a \left[\frac{17}{I_b(kA)} \frac{\gamma}{f_n}\right]^{\frac{1}{2}} \quad . \tag{32}$$

Note carefully that the length of pulse required for an e-folding contains the mass ratio $(m_i/m_e)^{\frac{1}{2}} >> 1$ while the required propagation distance does not. Hence, a long pulse propagated in the IFR will saturate at a very low level of hose but that saturated level will be reached very quickly in z.

VI. Non-Linear Development

Using the computational model of Section V, we may easily observe the non-linear behavior of the hose when the beam becomes displaced from the channel by a distance of order the beam radius ($\bar{Y} = O(1)$). We do this by returning to Equations (6) and (7) and applying the spread mass model. The result is that the first and third equations of set (25) are replaced by

$$U_i^{n+\frac{1}{2}} - U_i^{n-\frac{1}{2}} = 2i\Delta Z w_j \, (\bar{D} - Y_i) / \left[1 + \frac{1}{2}(Y_i - \bar{D})^2\right] N$$

$$V_j^{m+\frac{1}{2}} - V_j^{m-\frac{1}{2}} = 2j\Delta X w_j \, (\bar{Y} - D_i) / \left[1 + \frac{1}{2}(Y - D_i)^2 N\right] . \tag{33}$$

Using the same initial conditions as before but with a perturbation

$$\bar{Y}^o(X) = 0.005 \, H(X - X_o) \quad , \tag{34}$$

the results appear as in Figure 4. The initial perturbation has been chosen to lie well within the linear regime and, as expected, early growth appears as before. As $\bar{Y}$ reaches unity, however, growth slows and the wavelength in Z becomes very long. The reason for this is that the restoring force for the beam has become very non-linear and the system falls out of resonance. The instability, in effect, moves itself into a saturated regime by leaving the

vicinity of the channel. This is further dramatized by Figure 5 where $\bar{Y}_{max}$ has been plotted as a function of X for the perturbation of Equation (34). The upper curve results from the linearized Equations (25) and again shows pure exponential growth. The lower curve results from Equations (33) and shows the expected exponential growth in the linear regime with a later transition to saturated growth where $\bar{Y} \approx 3$. Each beam segment of $X \gtrsim 8$ would grow to this maximum $\bar{Y}$ and then damp away. At this displacement, however, the beam is mostly outside the channel so that other external forces (e.g., magnetic fields) may play an important role.

VII. Summary

The hose instability between a relativistic particle beam and an initially coaxial channel of un-neutralized ions has been examined. Analytic analysis of the rigid beam/rigid channel system shows absolute instability growing at a rate proportional to $(x^2 z)^{1/3}$. If mass spreading is applied to both the beam and the channel, the instability takes on a convective nature whose saturated growth can be described in the form $\exp\left[p(x - x_0)\right]$. Finally, the non-linear equations of motion were solved numerically and we find that hose growth saturates when the beam is displaced from the channel by a distance of the order of a beam radius. At this distance, the forces between beam and channel are weak and other forces can be important.

If one inserts typical values into Equations (31) and (32) one concludes that the ion hose instability as analyzed here should have been observed in ETA and ASTRON experiments where none was apparent. In fact, however, we have assumed that the channel has been totally ionized prior to the insertion of the beam so that the beam does no ionization itself. If this is not the case, as with a beam injected into cold gas, an ionization gradient exists from beam head to tail creating an additional spreading of betatron frequencies which detune the hose.

Finally, we may examine the experiment proposed by Fawley and Prosnitz[4] in which the beam from ETA (5 kA, 0.3 cm radius, γ = 10) is injected into one micron of Benzene in which a 5% neutralization has been created by illumination by a KrF laser. For this case the length of pulse required for one e-folding is 135. cm and the propagation distance for saturation is 18.2 cm. Except for self ionization effects, the ion hose should be readily discernable during the experiment.

References

1. R. J. Briggs and S. S. Yu, "Modeling Beam Front Dynamics at Low Gas Pressures," Lawrence Livermore National Laboratory report UCID-19399, May 13, 1982.

2. E. P. Lee, Phys. Fluids 21, 1327, (1978).

3. W. M. Fawley and E. P. Lee, "Modeling of Beam Focusing and Kink Instability for Colliding Relativistic Electron and Positron Beams," Lawrence Livermore National Laboratory report UCID-18584, February 8, 1980.

4. W. Fawley and D. Prosnitz, "Laser Photoionization and the IFR," Beam Physics Memo #25, January 25, 1982.

5506v/0416p

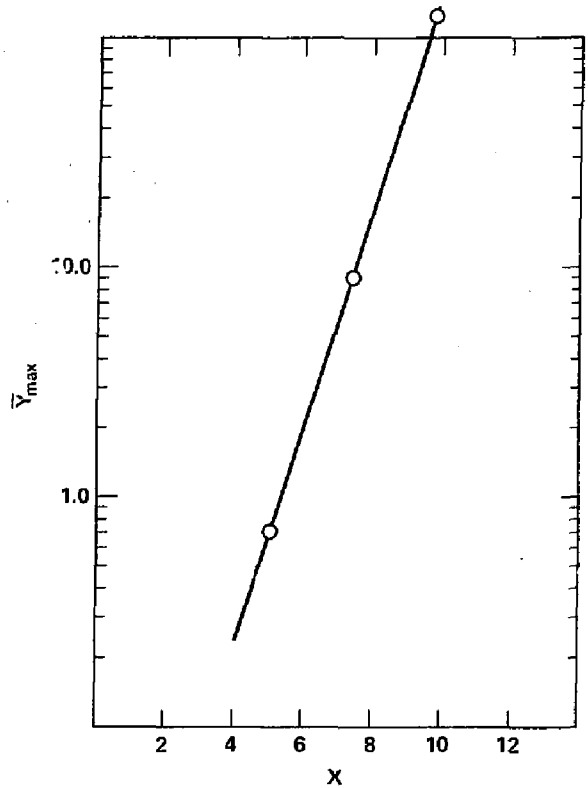

Fig. 1. Plot of $\overline{Y}_{max}$ versus X for saturated growth of IFR hose instability. Data points taken from numerical solution of linearized equations of motion.

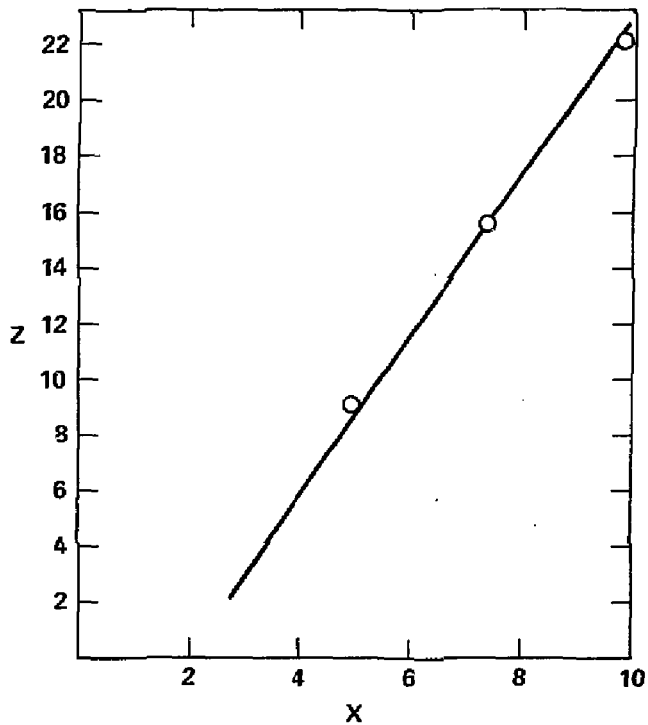

Fig 2. Plot of position in z versus position in X of saturated value of $\overline{Y}_{max}$. Data points taken from numerical solution of linearized equations of motion. Group velocity $\Delta X/\Delta Y = 0.379$.

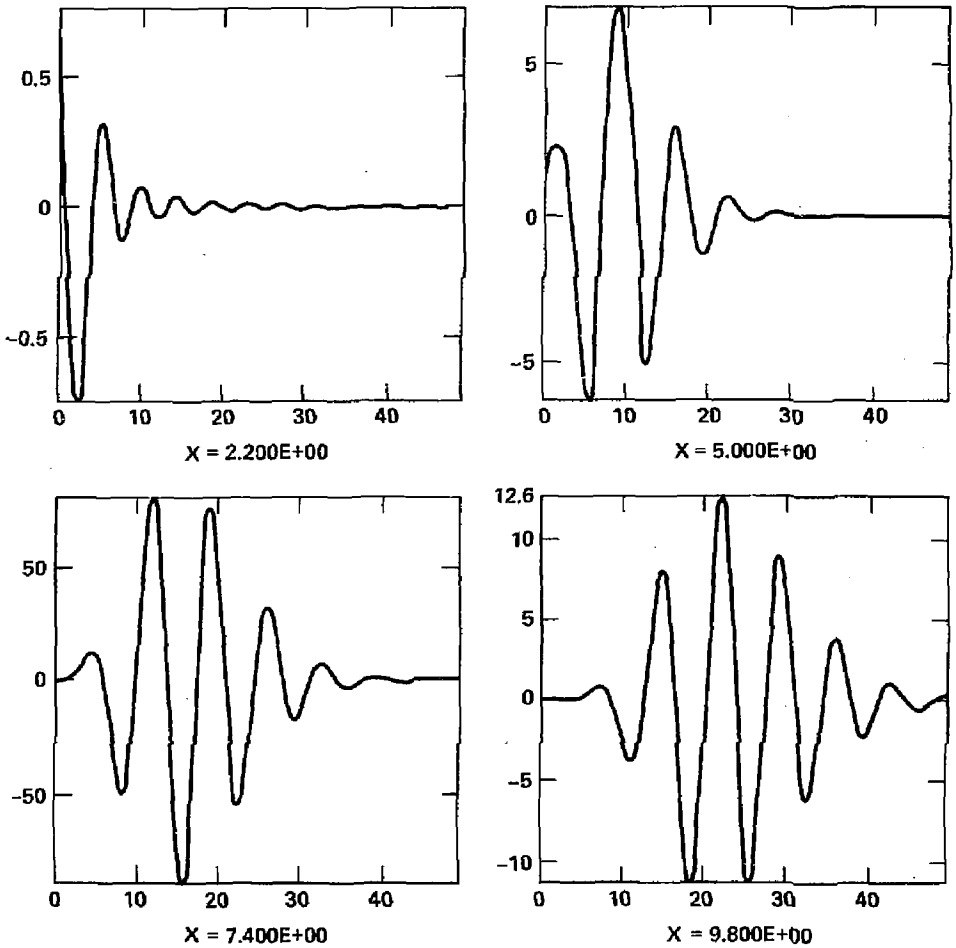

Fig. 3. Plots of $\overline{Y}$ versus z at fixed values of X with perturbation applied at X = 2. Initial disc (X = 2.2) shows no growth while following discs show initial growth and then a saturation and decay. Results obtained from linearized equations of motion.

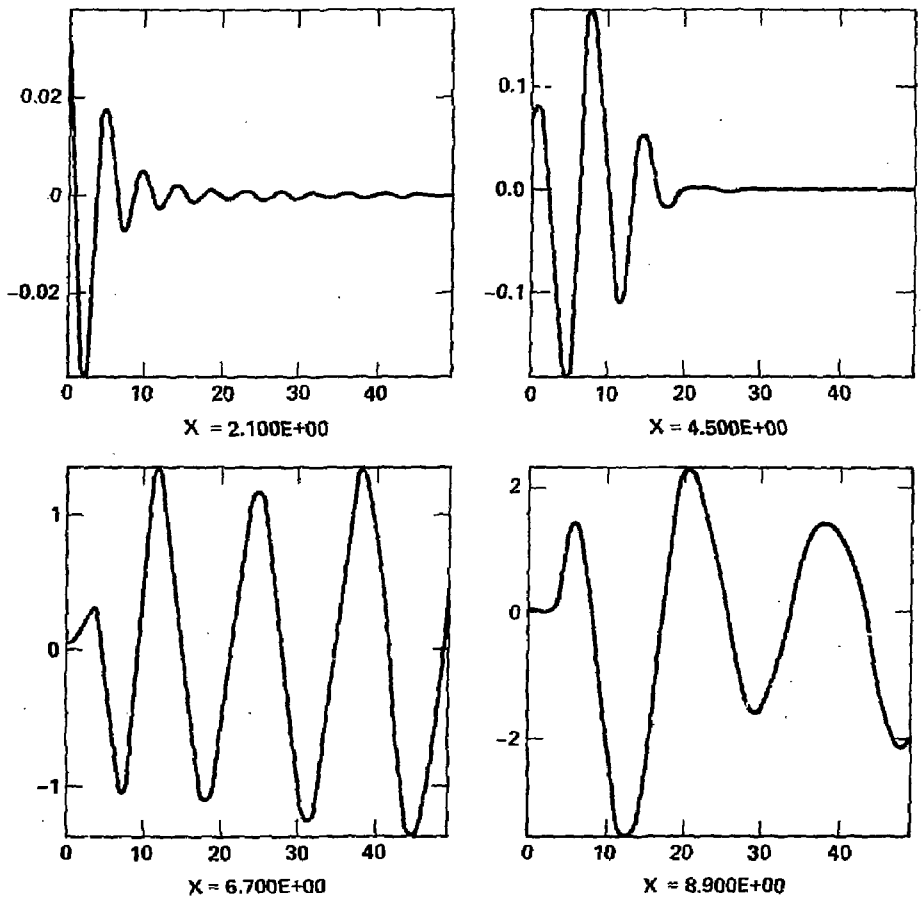

Fig. 4. Plots of $\overline{Y}$ versus z at fixed values of X using non-linear equations of motion. Note wavelength of instability grows longer as $\overline{Y}$ approaches unity.

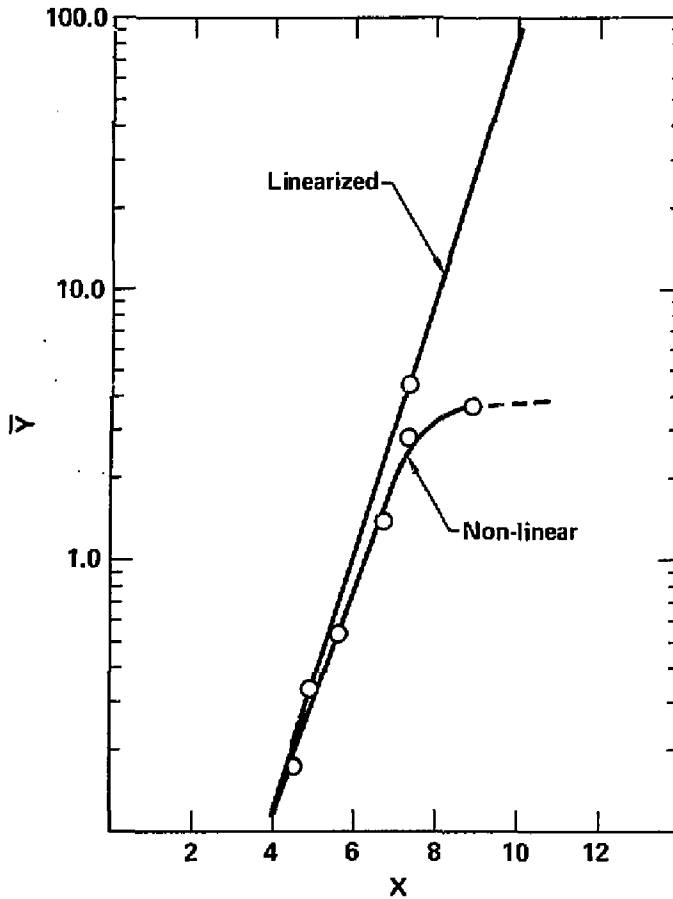

Fig. 5. Plot of $\overline{Y}_{max}$ versus X for linearized (top) and non-linear (bottom) equations of motion. Growth rate approaches zero as $\overline{Y}$ approaches order unity due to non-linear effects of finite beam and channel size.